Photoproduction of π^0 on Hydrogen using $e^+e^-(\gamma)$ detection mode with CLAS

Michael C. Kunkel,[1,2] Moskov J. Amaryan,[1,*] Igor I. Strakovsky,[3] James Ritman,[2,4] and Gary R. Goldstein[5]

[1] *Old Dominion University, Norfolk, VA 23529, USA*
[2] *Institut für Kernphysik, Forschungszentrum Jülich, 52424 Jülich, Germany*
[3] *The George Washington University, Washington, DC 20052, USA*
[4] *Institut für Experimentalphysik I, Ruhr-Universität Bochum, 44780 Bochum, Germany*
[5] *Tufts University, Medford, MA 02155, USA*

Abstract

We report the first high precision measurement of the exclusive π^0 photoproduction cross section, via the π^0 Dalitz decay and the $\pi^0 \to \gamma\gamma$ decay in which one γ undergoes e^+e^- pair conversion mode. The measurement was performed on a hydrogen target in a wide kinematic range with the CLAS setup at the Thomas Jefferson National Accelerator Facility. The measurement was performed using data from the reaction $\gamma p \to pe^+e^-X(\gamma)$ using a tagged photon beam spanning an energy interval from the "resonance" to the "Regge" regimes, i.e photon energies $E_\gamma = 1.25 - 5.55$ GeV. The final state particles p,e^+, ande^- were detected whereas the photon was inferred from energy and momentum conservation. This new data sample quadrupled the world database for π^0 photoproduction above $E_\gamma = 2$ GeV. Our data favors the Regge pole model and the constituent counting rule while disfavoring the Handbag model.

PACS numbers: 12.38.Aw, 13.60.Rj, 14.20.-c, 25.20.Lj

The rich pion-nucleon resonance spectrum for center-of-mass (c.m.) energies up to 2.5 GeV provides insights and challenges concerning the workings of the strong interaction through partial wave expansions, exchange potentials, non-relativistic quark models, and Quantum ChromoDynamics (QCD). Photoproduction of π^0 and η mesons has always enabled complementary investigations, constrained various models, and led to further insights. At the interface between the crowded low energy resonance production regime and the smooth higher energy, small angle behavior, traditionally described by Regge poles [1], lies a region in which hadronic duality interpolates the different excitation function behavior. Exclusive π photoproduction and π nucleon elastic scattering show this duality in a semi-local sense through Finite Energy Sum Rules (FESR) [2]. The connection to QCD is more tenuous for on-shell photoproduction of pions at small scattering angles, but the quark content can become manifest through large fixed angle dimensional counting rules [3], as well as being evident in semi-inclusive or exclusive electroproduction of pions, described through Transverse Momentum Distributions (TMDs) and Generalized Parton Distributions (GPDs).

The Regge pole description of photoproduction amplitudes has a long and varied history. For π^0 and η photoproduction, all applications rely on a set of known meson Regge poles. There are two allowed t-channel J^{PC} quantum numbers, the odd-signature (odd spin) 1^{--} (ρ^0, ω) and the 1^{+-} (b_1^0, h_1) Reggeons. Regge cut amplitudes are incorporated into some models and are interpreted as rescattering of on-shell meson-nucleon amplitudes. The phases between the different poles and cuts can be critical in determining the polarizations and the constructive or destructive interferences that can appear. Four distinct Regge models are considered here.

An early model developed by Goldstein and Owens [4] has the exchange of leading Regge trajectories with appropriate t-channel quantum numbers along with Regge cuts generated via final state rescattering through Pomeron exchange. The Regge couplings to the nucleon were fixed by reference to electromagnetic form factors, $SU(3)_{flavor}$, and low energy nucleon-nucleon meson exchange potentials. At the time, the range of applicability was taken to be above the resonance region and $|\, t \,| \leq 1.2\,\mathrm{GeV}^2$, where t is the squared four-momentum transfer. Here we will let the $|\, t \,|$ range extend to large $|\, t \,|$ in order to see the predicted cross section dips from the zeroes in the Regge residues. Because even signature partners (A_2, f_2) of the odd spin poles (ρ, ω) lie on the same trajectories, the Regge residues are required to have zeroes to cancel the even (wrong) signature poles in the physical region - these extra zeroes are called nonsense wrong signature zeroes (NWSZ) [5]. While the dip near $t \approx -0.5$ GeV^2 is present in the π^0 cross section data, it is absent in the beam asymmetry, Σ, measurement for π^0 and η photoproduction [6]. This is not explained by the standard form of the NWSZ Regge residues.

Quite recently, Mathieu *et al.* [7] from the Joint Physics Analysis Center (JPAC) (see also [8]), used the same set of Regge poles, but a simplified form of only ω -Pomeron cuts. They show that daughter trajectories are not significant as an alternative to the Regge cuts. However, to reproduce the lack of $t \approx -0.5$ GeV^2 dip in η photoproduction, they remove the standard wrong signature zero, i.e. the NWSZ. Donnachie and Kalashnikova [9] have included t-channel ρ^0, ω, and b_1^0 exchange, but not

* Corresponding author; mamaryan@odu.edu

the h_1 Reggeon, all with different parameterizations from Ref. [4]. They include $\omega, \rho \times$ Pomeron cuts, as well as $\omega, \rho \times \mathrm{f}_2$ lower lying cuts, which help to fill in the wrong signature zeroes of the ω, ρ Regge pole residues. The model of Laget and collaborators [10] included u-channel baryon exchange, which dominate at backward angles, along with elastic and inelastic unitarity cuts and a mechanism called "saturating, to fill the intermediate t range. "Saturating has all trajectories $\alpha(t) \rightarrow -1$ as a minimum. With these ingredients, the model is expected to describe the full angular range ($\theta_\pi = 0 \rightarrow \pi$), while the other models are good for more limited ranges of t [4, 7, 9]. Here, we examine how Regge phenomenology works for the energy range of 2.8 GeV $< \mathrm{E}_\gamma <$ 5.5 GeV.

In addition to Regge pole models, the introduction of the Handbag mechanism, developed by Kroll *et al.* [11], has provided complementary possibilities for the interpretation of hard exclusive reactions. In this approach, the reaction is factorized into two parts, one quark from the incoming and one from the outgoing nucleon participate in the hard sub-process, which is calculable using Perturbative Quantum ChromoDynamics (pQCD). The soft part consists of all the other partons that are spectators and can be described in terms of GPDs [12]. The Handbag model applicability requires a hard scale, which, for meson photoproduction, is only provided by large transverse momentum, which corresponds to large angle production, roughly for $-0.6 \leq \cos\theta_\pi \leq 0.6$, where θ_π is the pion polar production and in the c.m. frame. Here, we examined how the Handbag model may extend to the $\gamma p \rightarrow p\pi^0$ case proposed in [11]. The distribution amplitude for the quark+antiquark to π^0 is fixed by other phenomenology and leads to the strong suppression of the production cross section.

Binary reactions in QCD with large momentum transfer occur via gluon and quark exchanges between colliding particles. The constituent counting rules of Brodsky and Farrar [3] provide a simple recipe to predict the energy dependence of the differential cross sections of two-body reactions at large angles when t/s is finite and is kept constant. The lightest meson photoproduction was examined in terms of these counting rules [13–17]. As was first observed at SLAC by Anderson *et al.* [13], the reaction $\gamma p \rightarrow n\pi^+$ shows agreement with constituent counting rules that predict the cross section should vary as s^{-7}. The agreement extends down to $s = 6$ GeV^2 where baryon resonances are still playing a role. Here, we examined how applicable the counting rule is for $\gamma p \rightarrow p\pi^0$ up to $s = 10$ GeV^2.

Previous bremsstrahlung measurements of $\gamma p \rightarrow p\pi^0$, for $2 \leq E_\gamma \leq 18$ GeV (1964 – 1979) provided 451 data points for differential cross section $d\sigma/dt$ [18], have very large systematic uncertainties and do not have sufficient accuracy to perform comprehensive phenomenological analyses. A previous CLAS measurement of $\gamma p \rightarrow p\pi^0$, for $2.0 \leq E_\gamma \leq 2.9$ GeV, has an overall systematic uncertainty of 5% but only provided 164 data points for differential cross section $d\sigma/dt()$ [19].

The results described here are the first to allow a detailed analysis, bridging the nucleon resonance and high energy regions over a wide angular range, of exclusive pion photoproduction. By significantly extending the database they facilitate the examination of the resonance, "Regge", and wide angle QCD regimes of phenomenology. The broad range of c.m. energy, $\sqrt{s}$, is particularly helpful in sorting out the phenomenology associated with both Regge and QCD-based models of the nucleon [20].

In this work, we provide a large set of differential cross section values from $E_\gamma = 1.25 - 5.55$ GeV in laboratory photon energy, corresponding to a range of c.m. energies, $W = 1.81 - 3.33$ GeV. We have compared the Regge pole, the Handbag, and the constituent counting rule phenomenology with the new CLAS experimental information on $d\sigma/dt$ for the $\gamma p \rightarrow p\pi^0$ reaction above the "resonance" regime. As will be seen, this data set quadruples the world bremsstrahlung database above E_γ = 2 GeV and constrains the high energy phenomenology well with a previous CLAS measurement [19].

The experiment was performed during March-June, 2008 with the CLAS detector at Jefferson Laboratory [21] using a energy-tagged photon beam produced by bremsstrahlung from a 5.72 GeV electron beam provided by the CEBAF accelerator, which impinged upon a liquid hydrogen target, and was designated with the name $g12$. The experimental details are given in Ref. [22]. The reaction of interest is the photoproduction of neutral pions on a hydrogen target $\gamma p \rightarrow p\pi^0$, where the neutral pions decay into an $e^+e^-\gamma$ final state either due to external conversion, $\pi^0 \rightarrow \gamma\gamma \rightarrow e^+e^-\gamma$ or via Dalitz decay $\pi^0 \rightarrow \gamma^*\gamma \rightarrow e^+e^-\gamma$. Running the experiment at high beam current was possible due to the final state containing three charged tracks, p,e^+, e^-, as opposed to single prong charged track detection which impose limitations due to trigger and data acquisition restrictions.

Particle identification for the experiment was based on β vs. momentum$\times$charge. Lepton identification was based on a kinematic constraint to the π^0 mass. Once the data was skimmed for p, π^+, and π^- tracks, all particles that were π^+, π^- were tentatively assigned to be electrons or positrons based on their charge (for details, see Ref. [23]). After particle selection, standard $g12$ calibration, fiducial cuts and timing cuts were applied in the analysis [22].

Different kinematic fits were employed to cleanly identify the $\gamma p \rightarrow pe^+e^-(\gamma)$ reaction. They were applied to filter background from misidentified double pion production to the single π^0 production, to constrain the missing mass of entire final state to a missing photon and to ensure that the fit to the missing photon constrained the squared invariant mass of $e^+e^-(\gamma)$=$\mathrm{m}^2_{\pi^0}$. The values of the confidence levels cuts employed was determined using the statistical significance to get the best signal/background ratio. The confidence levels for each constraint were consistent between the $g12$ data and Monte-Carlo simulations. Monte-Carlo generation was performed using the PLUTO++ package developed for

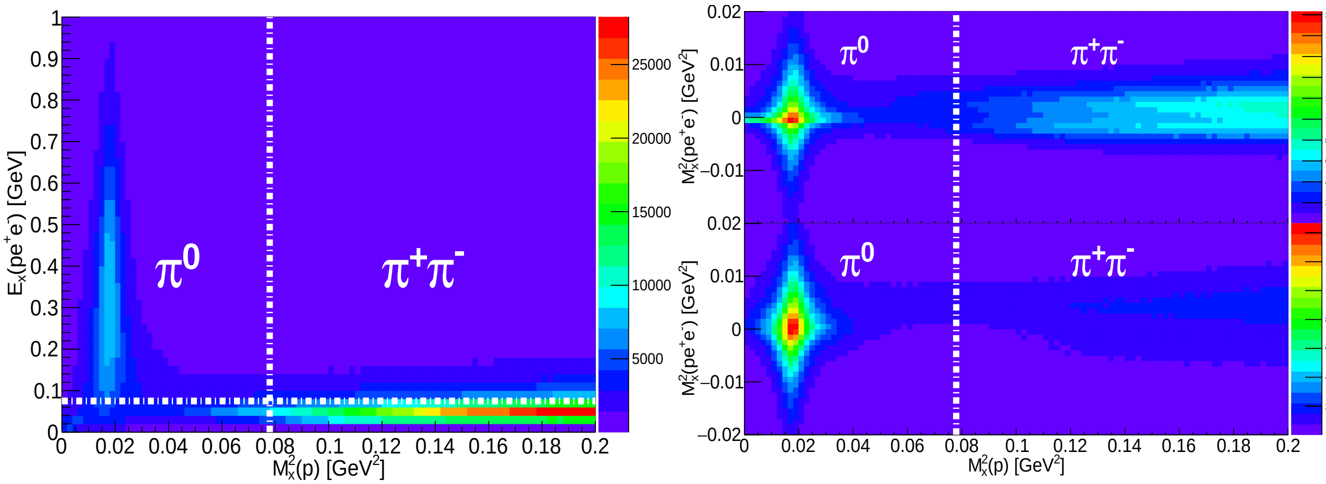

FIG. 1: (Color online)(left panel)Missing energy $\mathrm{E_X(pe^+e^-)}$ of all detected particles vs missing mass squared of the proton $\mathrm{M_x^2(p)}$. (Right panel) Missing mass squared of all detected particles $\mathrm{M_x^2(pe^+e^-)}$ vs missing mass squared of the proton $\mathrm{M_x^2(p)}$; (right-top panel) before applying the $\mathrm{E_X(pe^+e^-)} < 75$ MeV condition, (right-bottom panel) after applying the $\mathrm{E_X(pe^+e^-)} > 75$ MeV condition. The horizontal white dashed-dotted line depicted on the left panel illustrates the 75 MeV threshold used in this analysis. The vertical white dashed-dotted line depicts the kinematic threshold for $\pi^+\pi^-$ production.

the HADES Collaboration [24].

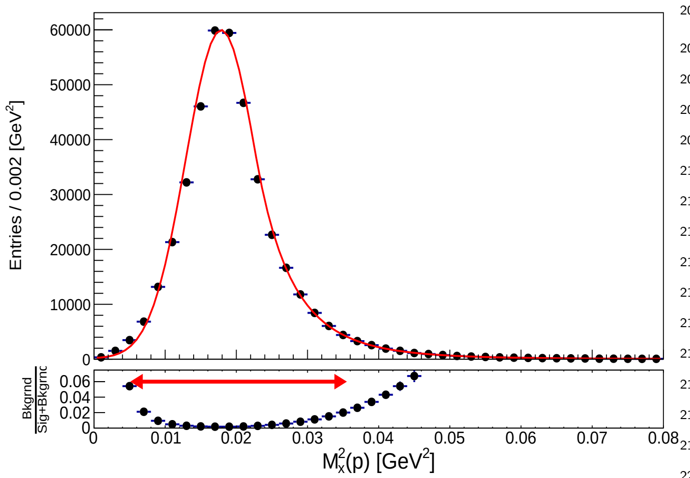

FIG. 2: (Color online) (top-panel) Peak of π^0 in the in the proton missing mass squared for events with $pe^+e^-(\gamma)$ in the final state. The red-solid line depicts the fit function (signal+background). (bottom-panel) Relative contributions of $\frac{\text{Background}}{\text{Signal+Background}}$. The red arrow indicates the cut placed on the $M_x^2(p)$ distribution to select π^0 events.

The remainder of the background was attributed to $\pi^+\pi^-$ events. To reduce the background further, a comparison of the missing mass squared off the proton, $\mathrm{M_x^2(p) = (P_\gamma + P_p - P_p^{'})^2}$, in terms of the four-momenta of the incoming photon, target proton, and final state proton, respectively, and the missing energy of detected system, $\mathrm{E_X(pe^+e^-)} = E_\gamma + E_p - E_p^{'} - E_{e^+} - E_{e^-}$, was performed, see Fig. 1. This comparison revealed that the majority of the $\pi^+\pi^-$ background has missing energy less than 75 MeV. To eliminate this background all events with a missing energy less than 75 MeV were removed.

The distribution of the proton missing mass squared for events with $pe^+e^-(\gamma)$ in the final state is shown in Fig. 2. A fit was performed with the Crystal Ball function [25, 26] for the signal, plus a 3rd order polynomial function for the background. The total signal+background fit is shown by the red solid line. The fit resulted in $M^2_{\pi^0} = 0.0179$ GeV^2 with a Gaussian width σ=0.0049 GeV^2. To select π^0 events, an asymmetric cut about the measured value was placed in the range 0.0056 GeV$^2 \leq M_x^2(p) \leq 0.035$ GeV^2. This cut range can be seen as the arrow in the bottom panel of Fig. 2 along with the ratio of background events to the total number of events. As shown in Fig. 2, the event selection strategy for this analysis led to a negligible integrated background estimated to be no more than 1.05%.

The total systematic uncertainty varied between 9% and 12% as a function of energy. The individual contributions came from particle efficiency, sector-to-sector efficiency, flux determination, missing energy cut, the kinematic fitting probabilities, target length, branching ratio, fiducial cut, and the z-vertex cut. The largest contributions to the systematic uncertainties were the sector-to-sector (4.4 – 7.1%), flux determination (5.7%), and the cut on the 1-C pull probability (1.6 – 6.1%). All systematic uncertainties and their determinations are described in Ref. [23].

As it was mentioned above there are two subprocesses that may led to the same final state $\pi^0 \to e^+e^-\gamma$. Both subprocesses were simulated in the Monte Carlo with their corresponding branching ratios and used to obtain cross sections from experimentally observed yield of neu-

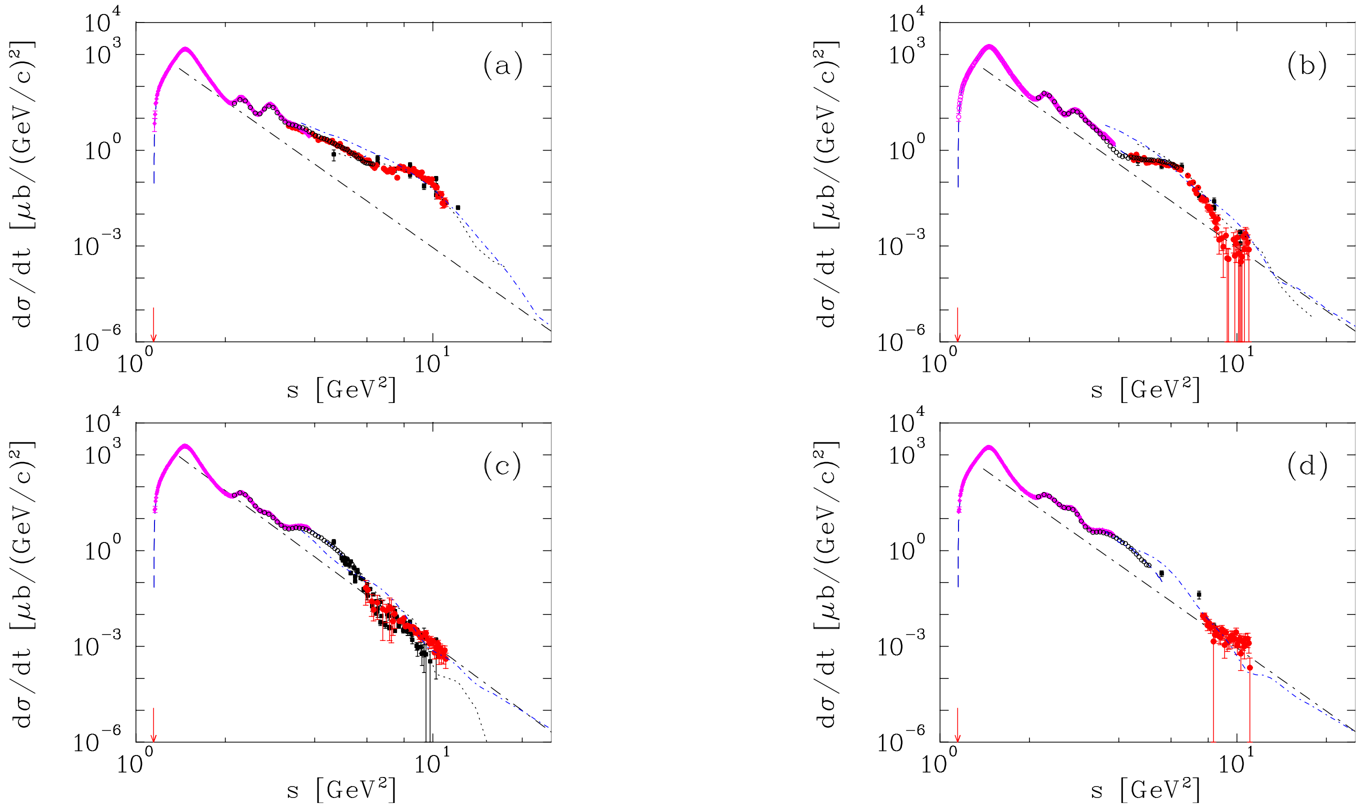

FIG. 3: (Color online) Differential cross section of $\gamma p \to\ p\pi^0 d\sigma/dt(s)$ at polar angles of (a) 50°, (b) 70°, (c) 90°, and (d) 110° in the c.m. frame as a function of c.m. energy squared, s. The red filled circles are the current $g12$ CLAS data. The recent tagged photon data are from previous CLAS Collaboration measurements [19] (black open circles) and the A2 Collaboration at MAMI [27] (magenta open diamonds with crosses), while the black filled squares are data from old bremsstrahlung measurements above $E_\gamma = 2$ GeV [18]. The plotted uncertainties are statistical. The blue dashed line corresponds to the SAID PWA PR15 solution (no new CLAS $g12$ data are used for the fit) [27]. The black dot-dashed lines are plotted as the best fit result of the power function s^{-n}, with $n = 6.89 \pm 0.26$, for the spectrum at 90°. The pion production threshold is shown as a vertical red arrow. The Regge results [4, 10] are given by the black dotted and the blue dash-dotted, respectively.

tral pions.

The new CLAS high statistics $\gamma p \to \pi^0 p$ cross sections from this analysis are compared in Figs. 3 and 4 with data from previous CLAS [19], bremsstrahlung DESY, Cambridge Electron Accelerator (CEA), and SLAC, and Electron Synchrotron at Cornell Univ. measurements [18], as well as lower c.m. energy MAMI A2 measurements [27]. The overall agreement is good, particularly with the previous CLAS data.

At higher energies (above $s \sim 6$ GeV^2) and large c.m. angles ($\theta_\pi \geq 90°$), the results are consistent with the s^{-7} scaling, at fixed t/s, as expected from the constituent counting rule [3]. The black dash-dotted line at 90° (Fig. 3) is a result of the fit of new CLAS $g12$ data only, performed with a power function $\sim s^{-n}$, leading to $n = 6.89 \pm 0.26$. Structures observed at 50° and 70° up to $s \sim$10 GeV^2 indicate that the constituent counting rule requires higher energies and higher $|t|$ before it can provide a complete description. In Figs. 4 and 5, the $d\sigma/dt$ results are shown along with predictions from Regge pole and cut [4, 7, 9, 10] models and the Handbag [11] model.

Below $|t|$ ∼0.6 GeV^2 there is a small difference between different Regge approaches. Overall, the Regge approximation becomes less applicable below $E_\gamma = 3$ GeV (Fig. 4). Note that some small dips start to appear around $|t| = 0.6$ GeV^2 ($\cos\theta_\pi = 0.6 - 0.8$) where the Regge models predict a dip. The dip at about $|t|$ ∼0.5 GeV^2 is best modeled by [7]. Prior to this measurement there was no indication of these dips. Note that the Regge amplitudes impose non-negligible constraints when continued down to the "resonance" region. Our data show another visible dip above $E_\gamma = 3.6$ GeV at around $|t|$ ∼2.6 GeV^2 and possible manifestation of another "possible new structure" around $|t|$ ∼5 GeV^2 for $E_\gamma > 4.1$ GeV, where the Regge models [4, 9, 10] predict wrong signature zeroes, this is where the Regge trajectories cross negative even integers. For the dominant vector meson Regge poles, these dips should appear at approximately $-t = 0.6$, 3.0, 5.0 GeV^2, which agrees with the data. The description of the π^0 photoproduction cross sections at largest $|t|$ requires improving the Regge model by including additional exchange mechanisms.

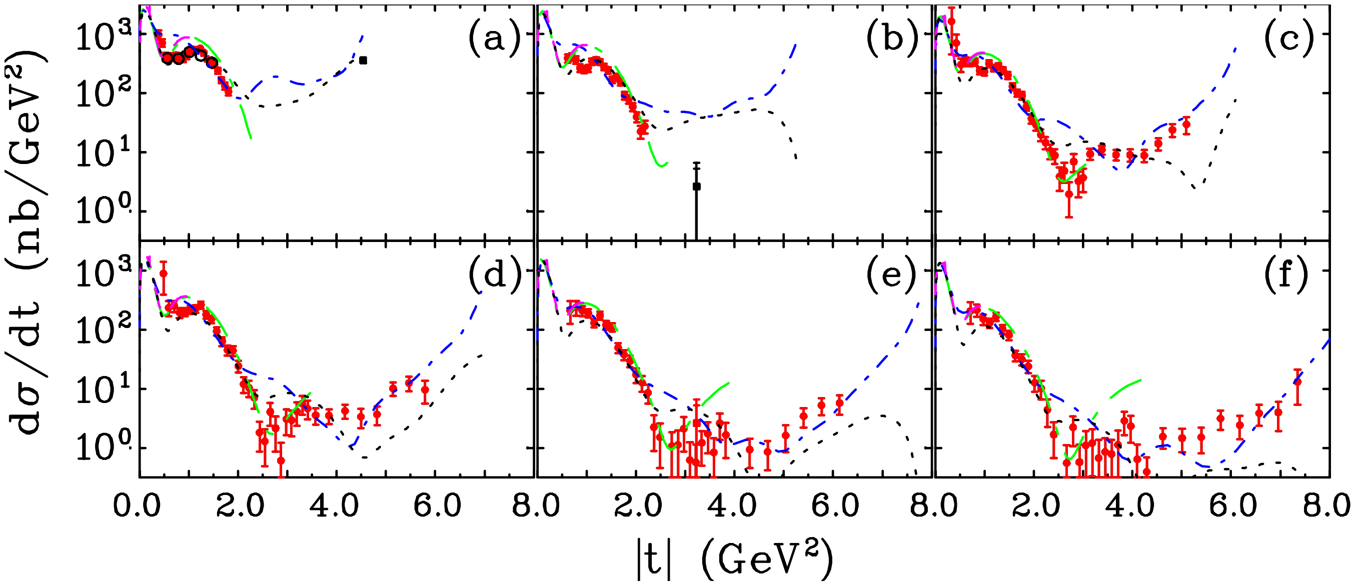

FIG. 4: (Color online) Samples of the π^0 photoproduction cross section, $d\sigma/dt$, off the proton versus $|t|$ above "resonance" regime. (a) $E_\gamma = 2825$ MeV and $W = 2490$ MeV, (b) $E_\gamma = 3225$ MeV and $W = 2635$ MeV, (c) $E_\gamma = 3675$ MeV and $W = 2790$ MeV, (d) $E_\gamma = 4125$ MeV and $W = 2940$ MeV, (e) $E_\gamma = 4575$ MeV and $W = 3080$ MeV, and (f) $E_\gamma = 4875$ MeV and $W = 3170$ MeV. Tagged experimental data are from the current CLAS $g12$ measurements (red filled circles) and a previous CLAS measurement [19] (black open circles). The plotted points from previously published bremsstrahlung experimental data above $E_\gamma = 2$ GeV [18] (black filled squares) are those data points within $\Delta E_\gamma = \pm 3$ MeV of the photon energy in the laboratory system indicated on each panel. The uncertainties plotted are only statistical. Regge results [4, 7, 9, 10] are given by black dotted, green long dash-dotted, magenta long dashed lines, and blue short dash-dotted, respectively.

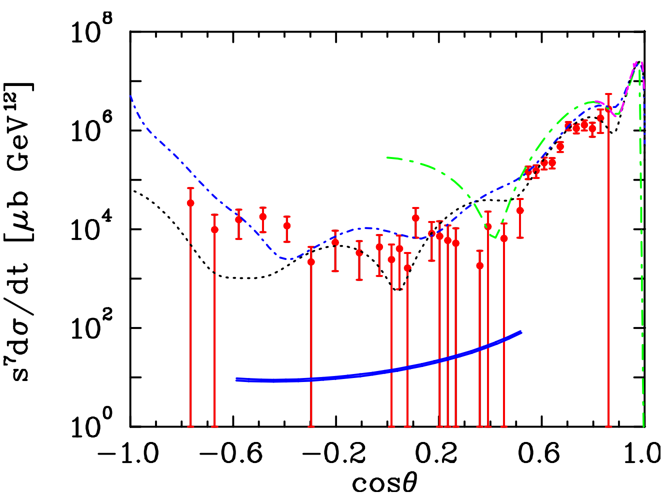

FIG. 5: (Color online) Differential cross section of π^0 photoproduction. The CLAS experimental data at $s = 11$ GeV^2 are from the current experiment (red filled circles). The theoretical curves for the Regge fits are the same as in Fig. 4 and the Handbag model by Kroll *et al.* [11] (blue double solid line).

Fig. 5 shows that the new CLAS data are orders of magnitude higher than the Handbag model prediction [11] for π^0 photoproduction below $s = 11$ GeV^2 (double solid line).

In this experiment a novel approach was employed based on the π^0 Dalitz decay mode. Although this decay mode has a branching fraction of only about 1%, the enhanced event trigger selectivity enabled the figure of merit to be sufficiently high in order to extend the existing world measurements into an essentially unmeasured *terra incognita* domain. Through the experiments described above, an extensive and precise data set (2030 data points) on the differential cross section for π^0 photoproduction from the proton has been obtained for the first time, except for a few points from previous measurements, over the range of $1.81 \le W \le 3.33$ GeV.

Measurements were performed in the reaction $\gamma p \to pe^+e^-X(\gamma)$ using a tagged photon beam spanning the energy interval covered by the "resonance" and "Regge" regimes. The measurements obtained here have been compared to existing data. The overall agreement is good, while the data provided here quadrupled the world bremsstrahlung database above $E_\gamma = 2$ GeV and covered the previous reported energies with finer resolution. This new and greatly expanded set of data provides strong confirmation of the basic features of models based on Regge poles and cuts. There is enough precision to discriminate among the distinct components of those models. Guided by this data, extensions of models and improved parameterization is now possible. From another perspective, the wide angle data agree with the pQCD based constituent counting rules. Yet a significant paradox now appears: the wide angle data disagree - by orders of magnitude - with a handbag model that combines pQCD with the soft region represented by GPDs. This is an important result that needs to be better understood.

The results presented in this paper form part of the Ph.D. dissertation of Michael C. Kunkel [28]. We thank Stanley Brodsky, Alexander Donnachie, Peter Kroll, Jean-Marc Laget, Vincent Mathieu, and Anatoly Radyushkin for discussions of our measurements. We would like to acknowledge the outstanding efforts of the staff of the Accelerator and the Physics Divisions at Jefferson Lab that made the experiment possible. This work was supported in part by the Italian Istituto Nazionale di Fisica Nucleare, the French Centre National de la Recherche Scientifique and Commissariat à l'Energie Atomique, the United Kingdom's Science and Technology Facilities Council (STFC), the U. S. DOE and NSF, and the National Research Foundation of Korea. The Southeastern Universities Research Association (SURA) operates the Thomas Jefferson National Accelerator Facility for the US DOE under contract DEAC05–84ER40150.

[1] J. P. Ader, M. Capdeville, and P. Salin, Nucl. Phys. B **3**, 407 (1967).
[2] H. K. Armenian, G. R. Goldstein, J. P. Rutherfoord, and D. L. Weaver, Phys. Rev. D **12**, 1278 (1975).
[3] S. J. Brodsky and G. R. Farrar, Phys. Rev. Lett. **31**, 1153 (1973).
[4] G. R. Goldstein and J. F. Owens, Phys. Rev. D **7**, 865 (1973).
[5] C. B. Chiu, Nucl. Phys. B **30**, 477 (1971).
[6] H. Al Ghoul *et al.* [GlueX Collaboration], Phys. Rev. C **95**, no. 4, 042201 (2017).
[7] V. Mathieu, G. Fox, and A. P. Szczepaniak, Phys. Rev. D **92**, no. 7, 074013 (2015); J. Nys *et al.* [JPAC Collaboration], Phys. Rev. D **95**, no. 3, 034014 (2017).
[8] V. L. Kashevarov, M. Ostrick, and L. Tiator, Phys. Rev. C **96**, 035207 (2017).
[9] A. Donnachie and Y. S. Kalashnikova, Phys. Rev. C **93**, no. 2, 025203 (2016).
[10] J. M. Laget, Phys. Lett. B **695**, 199 (2011);
[11] H. W. Huang and P. Kroll, Eur. Phys. J. C **17**, 423 (2000); H. W. Huang, R. Jakob, P. Kroll, and K. Passek-Kumericki, Eur. Phys. J. C **33**, 91 (2004); M. Diehl and P. Kroll, Eur. Phys. J. C **73**, no. 4, 2397 (2013).
[12] X. D. Ji, Phys. Rev. D **55**, 7114 (1997); A. V. Radyushkin, Phys. Lett. B **380**, 417 (1996); A. V. Radyushkin, Phys. Rev. D **56**, 5524 (1997); D. Müller, D. Robaschik, B. Geyer, F.-M. Dittes, and J. Horejsi, Fortsch. Phys. **42**, 101 (1994).
[13] R. L. Anderson, D. Gustavson, D. Ritson, G. A. Weitsch, H. J. Halpern, R. Prepost, D. H. Tompkins, and D. E. Wiser, Phys. Rev. D **14**, 679 (1976).
[14] D. A. Jenkins and I. I. Strakovsky, Phys. Rev. C **52**, 3499 (1995).
[15] L. Y. Zhu *et al.* [Jefferson Lab Hall A Collaboration], Phys. Rev. Lett. **91**, 022003 (2003).
[16] W. Chen *et al.* [CLAS Collaboration], Phys. Rev. Lett. **103**, 012301 (2009).
[17] K. J. Kong, T. K. Choi, and B. G. Yu, Phys. Rev. C **94**, no. 2, 025202 (2016).
[18] The Durham HEP Reaction Data Databases (UK) (Durham HepData): http://durpdg.dur.ac.uk/hepdata/reac.html.
[19] M. Dugger *et al.* [CLAS Collaboration], Phys. Rev. C **76**, 025211 (2007).
[20] P. Kroll, Eur. Phys. J. A **53**, no. 6, 130 (2017) and references therein.
[21] B. A. Mecking *et al.* [CLAS Collaboration], Nucl. Intrum. Methods A503, 513 (2003).
[22] G12 experimental group, CLAS-NOTE 2017 - 002, 2017 `https://misportal.jlab.org/ul/Physics/Hall-B/clas/viewFile.cfm/2017-002.pdf?documentId=756`.
[23] M. C. Kunkel, CLAS-NOTE 2017 - 005, 2017 `https://misportal.jlab.org/ul/Physics/Hall-B/clas/viewFile.cfm/2017-005.pdf?documentId=767`.
[24] I. Frohlich *et al.*, PoS ACAT, 076 (2007) [arXiv:0708.2382 [nucl-ex]].
[25] M. Oreglia, SLAC Stanford - SLAC-236 (80,REC.APR. 81) 226p; Ph. D. Thesis, SLAC, 1980.
[26] T. Skwarnicki, DESY-F31-86-02, DESY-F-31-86-02; Ph. D. Thesis, Inst. Nucl. Phys. Cracow, Poland, 1986.
[27] P. Adlarson *et al.* [A2 Collaboration at MAMI], Phys. Rev. C **92**, no. 2, 024617 (2015).
[28] M. C. Kunkel, Ph. D. Thesis, 2014 `https://www.jlab.org/Hall-B/general/thesis/Kunkel_thesis.pdf`.